Scanning Microscopy

Volume 3 | Number 3 Article 22

9-18-1989

Scanning Electron Microscopy of Lung Following Alpha Irradiation

C. L. Sanders
Pacific Northwest Laboratory

K. E. Lauhala
Pacific Northwest Laboratory

K. E. McDonald
Pacific Northwest Laboratory

Scanning Microscopy, Vol. 3, No. 3, 1989 (Pages 907-918) 0891-7035/89$3.00+.00
Scanning Microscopy International, Chicago (AMF O'Hare), IL 60666 USA

SCANNING ElECTRON MICROSCOPY OF LUNG FOLLOWING ALPHA IRRADIATION

C.L. Sanders*, K.E. Lauhala, and K.E. McDonald

Biology and Chemistry Department, Pacific Northwest Laboratory,
Richland, WA 99352

(Received for publication January 29, 1989, and in revised form September 18, 1989)

Abstract

Pulmonary aggregation of inhaled $^{239}PuO_2$ particles leads to a cellular evolution of focal inflammation, fibrosis, epithelial dysplasia and lung tumor formation. Female Wistar rats were exposed to an aerosol of high-fired $^{239}PuO_2$ (initial lung burden, 3.9 kBq) and the lungs examined at intervals from 1 day to 700 days after exposure by light and scanning electron microscopy and autoradiography. Peribronchiolar Pu particle aggregation increased with time, resulting in well-defined focal inflammatory lesions after 120 days and fibrotic lesions after 180 days. A generalized hypertrophy and hyperplasia of nonciliated bronchiolar cells was seen at 15 days and type II cell hyperplasia by 30 days after exposure. Focal dysplastic changes in type II alveolar epithelium and terminal nonciliated bronchiolar epithelium preceded carcinoma formation. Alveolar bronchiolarization was first noted at 120 days, squamous metaplasia at 210 days, squamous carcinoma at 270 days and adenocarcinoma at 600 days after exposure.

Key Words: Scanning electron microscopy, pathology, lung, plutonium, autoradiography.

*Address for correspondence:
C.L. Sanders
Pacific Northwest Laboratory
Biology and Chemistry Department
Richland, WA 99352
Phone No. (509) 376-1015

Introduction

Lung cancer in the rat is a common long-term effect of moderate to high levels of inhaled $^{239}PuO_2$ (Sanders, et al., 1988a). A significant incidence of lung tumors is seen only at lifetime, total lung doses greater than 1 Gy; a maximal lung tumor incidence of about 80% is seen at a lung dose of 8 Gy. Lung tumors most frequently seen in rats following inhalation of transuranics include squamous cell carcinoma and adenocarcinoma, which probably are derived from terminal bronchiolar epithelium and/or type II alveolar epithelium (Sanders et al., 1986, 1988a, 1988b; Masse, 1980; Lisco, 1959). The formation of large peribronchiolar Pu particle aggregates result in average of about 1 cGy/day to small focal areas of contiguous alveolar and bronchiolar epithelium at periods greater than 6 months after inhalation. These overlapping alpha particle radiation zones appear to be required for subsequent development of lung tumors (Sanders et al., 1988b). Pu particle aggregation leads to a cellular evolution of focal inflammation, fibrosis, epithelial hyperplasia and metaplasia, and lung tumor formation at total lung doses greater than 1 Gy.

Morphological evidence for multiple steps in the progression to malignant tumors of the lung from inhaled Pu is well established. This histopathological progression has been examined in studies of Pu distribution (Rhoads et al., 1982), cell proliferation (Rhoads et al., 1983), morphometry (Rhoads et al., 1981), and ultrastructure (Sanders et al., 1971). Pathological changes in irradiated lung have been described using transmission and scanning electron microscopy (SEM) (Woodruff et al., 1977; Maisin et al., 1982; Nicholls et al., 1986; Sanders et al., 1971). Scanning electron microscopic autoradiography has been used to visualize and quantitate the distribution of inhaled $^{239}PuO_2$ particles in alveolar and bronchiolar regions of lung (Lauhala et al., 1988; Sanders et al., 1989). This paper reports on the histopathological lesions leading to lung tumor formation from the perspective of the scanning electron microscope.

Materials and Methods

Ninety-nine young adult, SPF, female Wistar rats were given a single, nose-only exposure to an aerosol of ^{169}Yb, $^{239}PuO_2$ in groups of 33 rats; 40 rats were sham-exposed. The aerodynamic median activity diameter of the aerosol was 2.1 micrometers, with a geometrical standard deviation of 2.0. Initial lung burden (ILB) of ^{239}Pu in individual rats was

Table 1. Incidence of pulmonary proliferative lesions following inhalation of $^{239}PuO_2$; values are percentages of 5 rats per group, except for 4 rats at 700 days, with specified lesions. Only one sham-exposed rat developed a lesion, alveolar bronchiolarization at 500 days after exposure.

Time after Inhalation (days)	Incidence of Pulmonary Lesions (percent)			
	Alveolar bronchiolarization	Squamous Metaplasia	Adeno-carcinoma	Squamous Carcinoma
1	0	0	0	0
15	0	0	0	0
28	0	0	0	0
60	0	0	0	0
90	0	0	0	0
120	20	0	0	0
150	0	0	0	0
180	40	0	0	0
210	80	20	0	0
240	40	0	0	0
270	60	0	0	20
300	100	0	0	0
350	100	0	0	0
400	60	40	0	0
450	100	20	0	20
500	80	20	0	20
550	60	0	0	40
600	60	20	20	20
650	80	20	20	20
700*	50	0	25	0

*four rats in the final group.

determined at 14 days post-exposure by whole body counting of ^{169}Yb activity. The activity ratio of $^{169}Yb/^{239}Pu$ was 0.40. The contribution of ^{169}Yb gamma-irradiation to the total lung dose was less than 0.05%. ILB for ^{239}Pu was 3.9 + 1.2 kBq. Radiation dose to the entire lung was calculated based on ILB and time to sacrifice after exposure using a two-exponent lung clearance function and a lung weight of 1.6 grams (Sanders et al., 1986, 1988b). About 80% of ^{239}Pu was cleared from the lung with a half-life of 20 days and 20% was cleared with a half-life of 200 days. Groups of five exposed rats and two sham-exposed rats were examined with light and scanning electron microscopes at 20 time periods ranging from 1 day to 700 days post-exposure (Table 1).

Rats were anesthetized with intraperitoneally injected sodium barbitol. At the time of sacrifice, the trachea was exposed and cannulated with a 14-gauge needle and perfused with McDowell-Trump's fixative (McDowell and Trump, 1976) in situ for 20 minutes at 25 cm of water pressure. The trachea was then tied off and the lung immersed in fixative at 4°C. The lung lobes were removed from the main stem bronchi and prepared for examination by light microscopy (LM) and SEM. Random portions of the left lobe were dehydrated and embedded in Lx-112 resin. One micrometer thick Lx-112 resin sections were cut on an LKB ultramicrotome with a diamond knife and stained with Richardson's stain and basic fuchsin or covered with Ilford K-5 liquid photographic emulsion (Ilford Limited Mobberley Cheshire, England) and exposed for 4 weeks. Slides Richardson's and basic fuchsin. The cardiac lobe was prepared for SEM and SEM autoradiographic examination (Lauhala et al., 1988; Sanders et al., 1988c).

Results

Plutonium particles were widely dispersed throughout the pulmonary region at 1 and 15 days after exposure (Figure 1 A). Early evidence of $^{239}PuO_2$ particle aggregation was seen by 28 days. These "hot-spot" regions in alveoli on SEM autoradiograms contained a concentration of alpha tracks and alpha stars along with numerous single reduced silver grains, perhaps arising from secondary delta rays. Regions of particle concentration became more evident from 60-180 days after exposure, due to both a clearance of particles from other alveolar regions and an apparent concentration effect in a few focal regions. By 120 days, the density of reduced silver grains in this high-dose area of particle concentration was so great in some cases that they covered most of the underlying tissue. Focal plutonium particle aggregates were more frequent and extensive by 200-300 days (Figures 1 B and 1 C). Aggregates were seen most often in more peripheral and

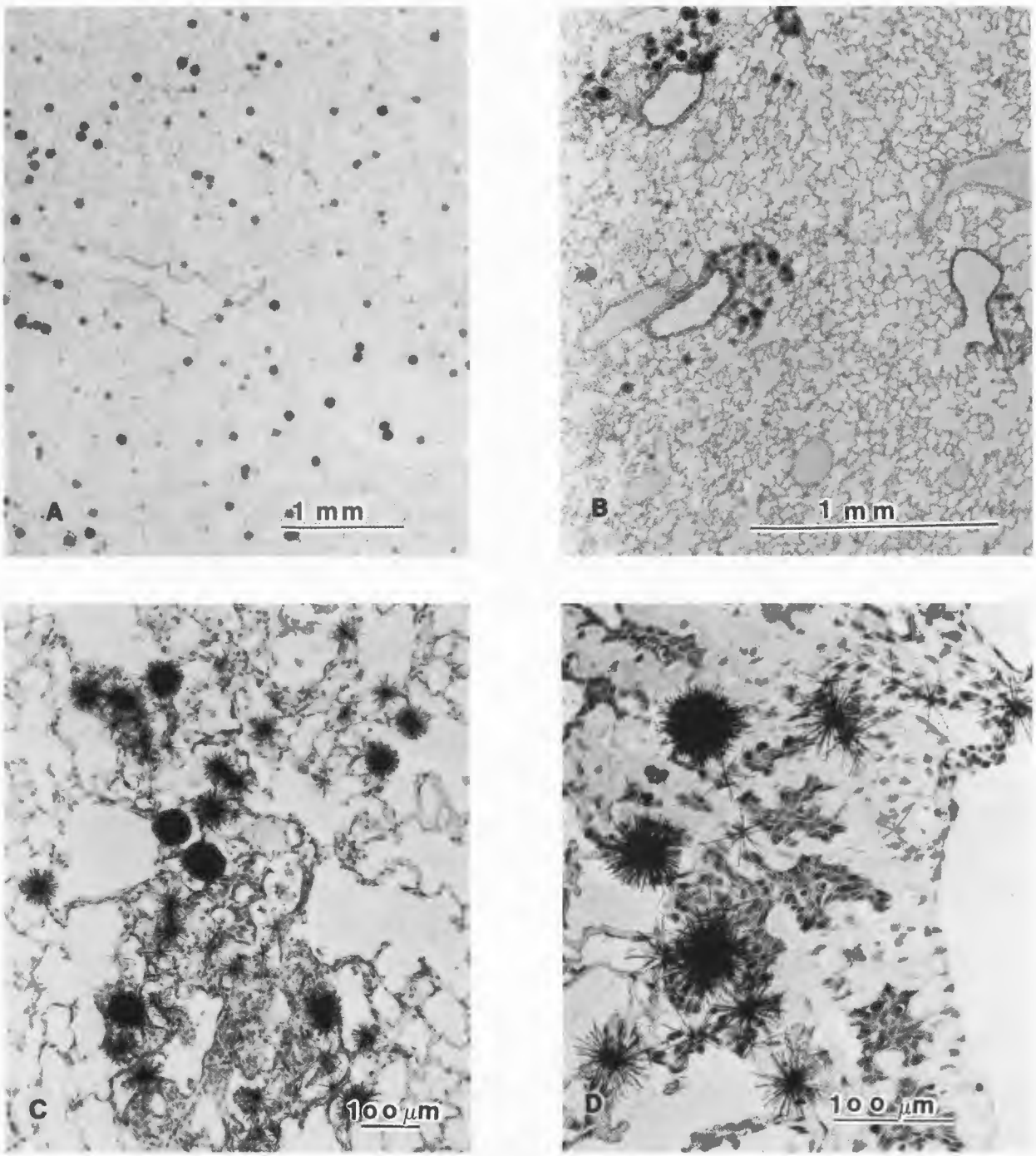

Figure 1. Light microscopic autoradiographs of lung at (A) 1 day, (B) 270 days, (C) 300 days and (D) 450 days after inhalation of $^{239}PuO_2$ showing aggregation of Pu particles around bronchioles in (B), inflammatory lesion associated with Pu particle aggregate in (C), and Pu particle aggregate associated with subplural foci of alveolar fibrosis and squamous metaplasia in (D).

peribronchiolar areas of the lung. Focal inflammatory, fibrotic, and epithelial dysplastic lesions were associated with the formation of large Pu aggregates (Figures 1 D and 2 D). Alpha tracks and stars are readily seen in SEM autoradiographs of lung. SEM autoradiographs, used in conjunction with light microscopic autoradiography provides an excellent view of the spatial alpha track distribution in the alveoli (Figure 2 A) and can be used to quantify the distribution of Pu particles on the surface of the

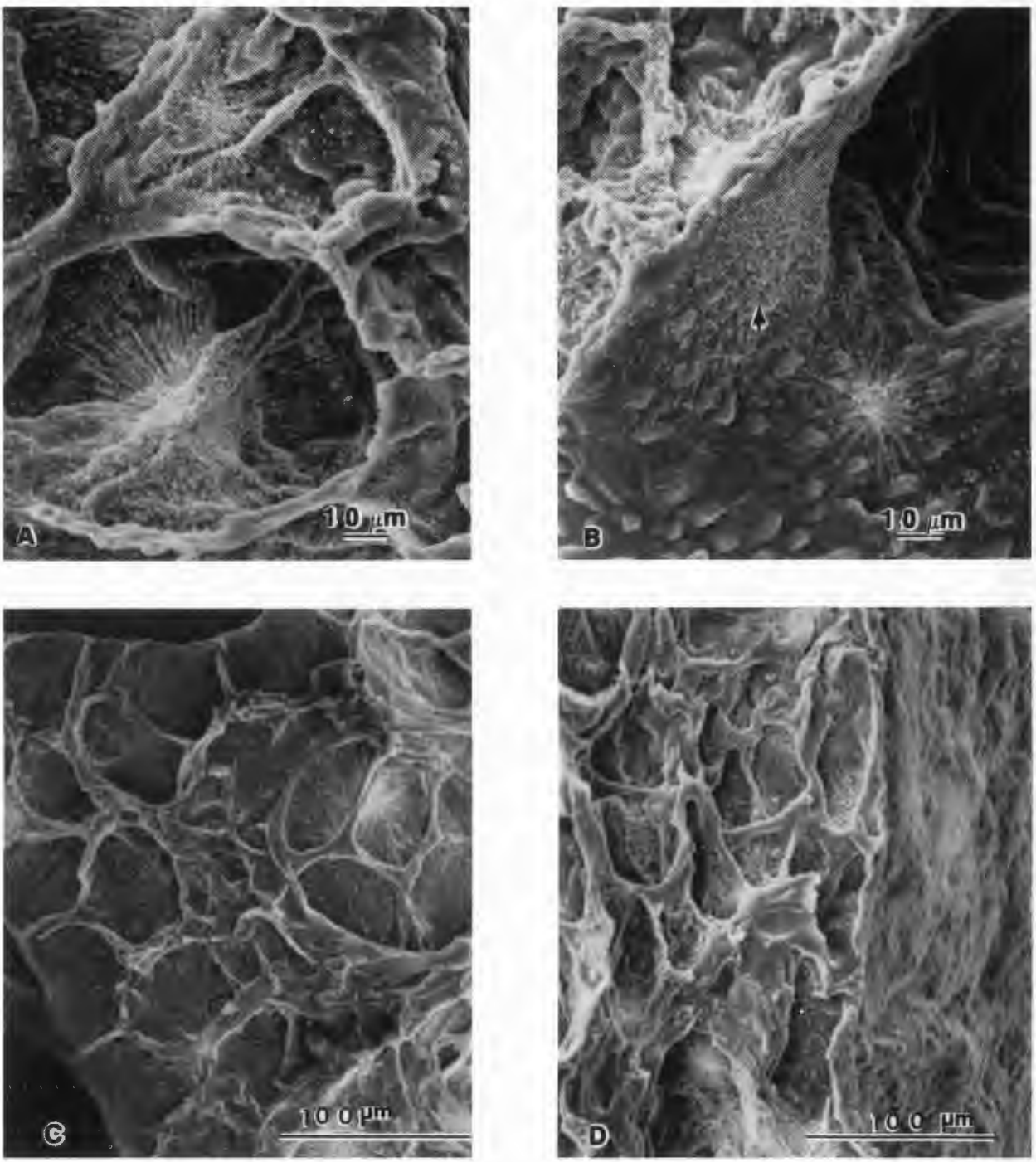

Figure 2. SEM autoradiographs showing **(A)** alveolar distribution of alpha stars from Pu particles at 60 days; **(B)** distribution of alpha stars from Pu particles on the surface of a bronchiole and in a peribronchiolar alveolus (arrow) at 60 days; (C) the distribution of alpha stars from Pu particles found in alveoli position directly over the surface of a bronchiole at 210 days; and **(D)** aggregation of Pu particles in a subpleural region of the lung at 60 days, after inhalation of $^{239}PuO_2$.

bronchioles and in alveolar peribronchiolar regions of the lung (Figures 2 B and 2 C).

In the rat, epithelial cells of the terminal bronchioles are normally comprised of about half nonciliated and half ciliated cells (Figure 3 A). Nonciliated cells underwent a generalized hypertrophy and hyperplasia at 15-28 days after exposure (Figures 3 B and 3 C), returning to normal in most areas within a few

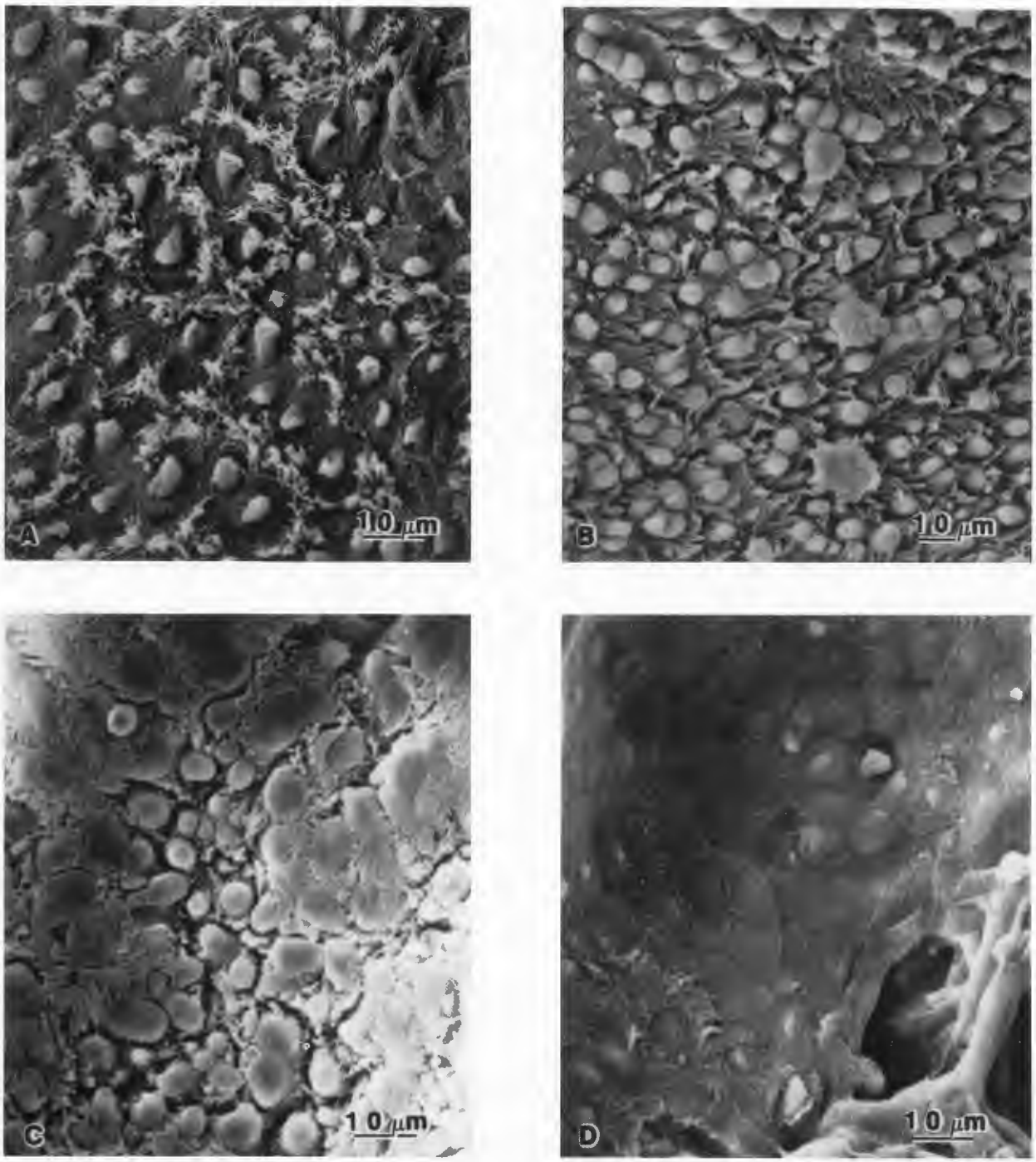

Figure 3. (A) Normal terminal bronchiolar epithelium at 60 days after sham exposure. Note the normal distribution of ciliated and nonciliated epithelial cells. (B) Hyperplasia and hypertrophy of nonciliated cells in the terminal bronchiolar epithelium at 15 days; (C) hyperplasia and marked hypertrophy of nonciliated cells in the terminal bronchiolar epithelium at 28 days; and (D) squamous metaplasia in the terminal bronchiolar epithelium at 350 days, after inhalation of $^{239}PuO_2$.

months. Squamous metaplasia of terminal bronchioles was seen as early as 180 days postexposure (Figure 3 D) and was most severe in bronchioles associated with severe fibrosis due to Pu particle aggregation (shown later in Figures 7 A and 7 B).

The formation of $^{239}PuO_2$ aggregates was related in space and in time to the development of focal inflammatory lesions and later fibrotic lesions in the

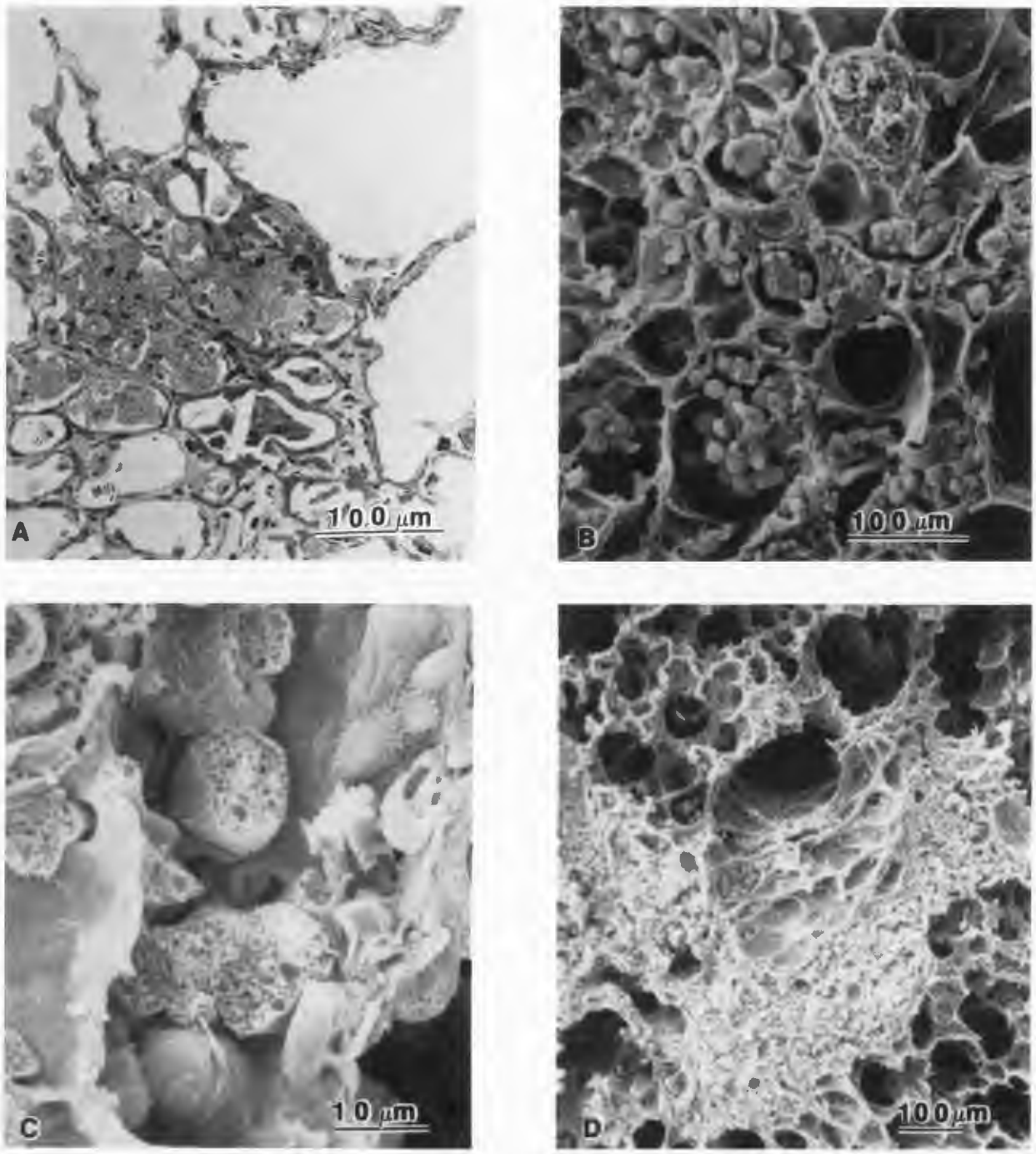

Figure 4. **(A)** A small foci of inflammatory cells (mostly histiocytes) in the alveolar region of the lung at 210 days; **(B)** SEM view of focal alveolar inflammatory lesion at 240 days; (C) higher magnification view of inflammatory lesion showing highly vaculolized histiocytes at 270 days; and **(D)** alveolar hyalinization and focal fibrosis at 450 days, after inhalation of $^{239}PuO_2$.

same areas. Only occasional single macrophages were found in alveoli at 1-28 days after exposure. A few small regions of focally diffuse concentrated inflammatory cells were seen at 60 and 90 days. Focal inflammatory lesions were more common by 210 to 270 days after exposure comprised of histiocytes and other mononuclear inflammatory cells (Figures 4 A, 4 B, and 4 C). Large groupings of inflammatory cells were seen in individual alveoli comprising the focal lesion (usually 10-30 alveoli in diameter). The more

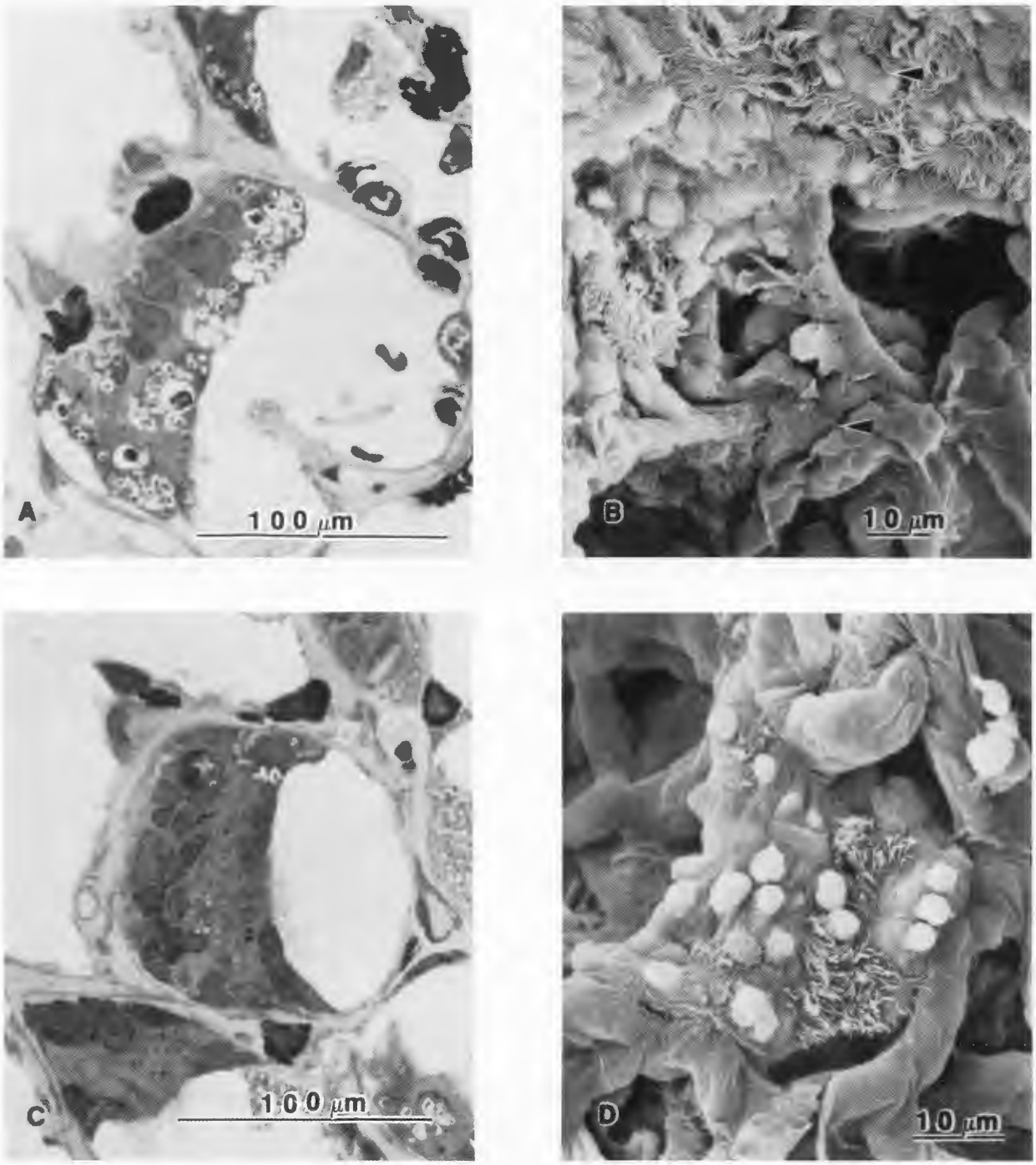

Figure 5. (A) Focal hyperplasia of type 2 alveolar epithelium at 210 days; (B) SEM view of type 2 alveolar epithelial hyperplasia (arrows) near a terminal bronchiole at 270 days; (C) alveolar bronchiolarization at 300 days; and (D) SEM view of alveolar bronchiolarization at 700 days, after inhalation of $^{239}PuO_2$. Note presence of ciliated and nonciliated epithelium in (C).

severe lesions were comprised of large numbers of necrotic cells, cell debris, and in a few cases with mucous from nearby bronchioles. The inflammatory foci became less cellular as the fibrotic process evolved, with fewer inflammatory cells and thickening of alveolar walls. Alveolar capillaries in regions of inflammation were non-functional with smooth alveolar walls and lack of RBCs. Advanced fibrotic lesions were comprised of collapsed alveolar walls, preceded by a gradual decrease in alveolar space size

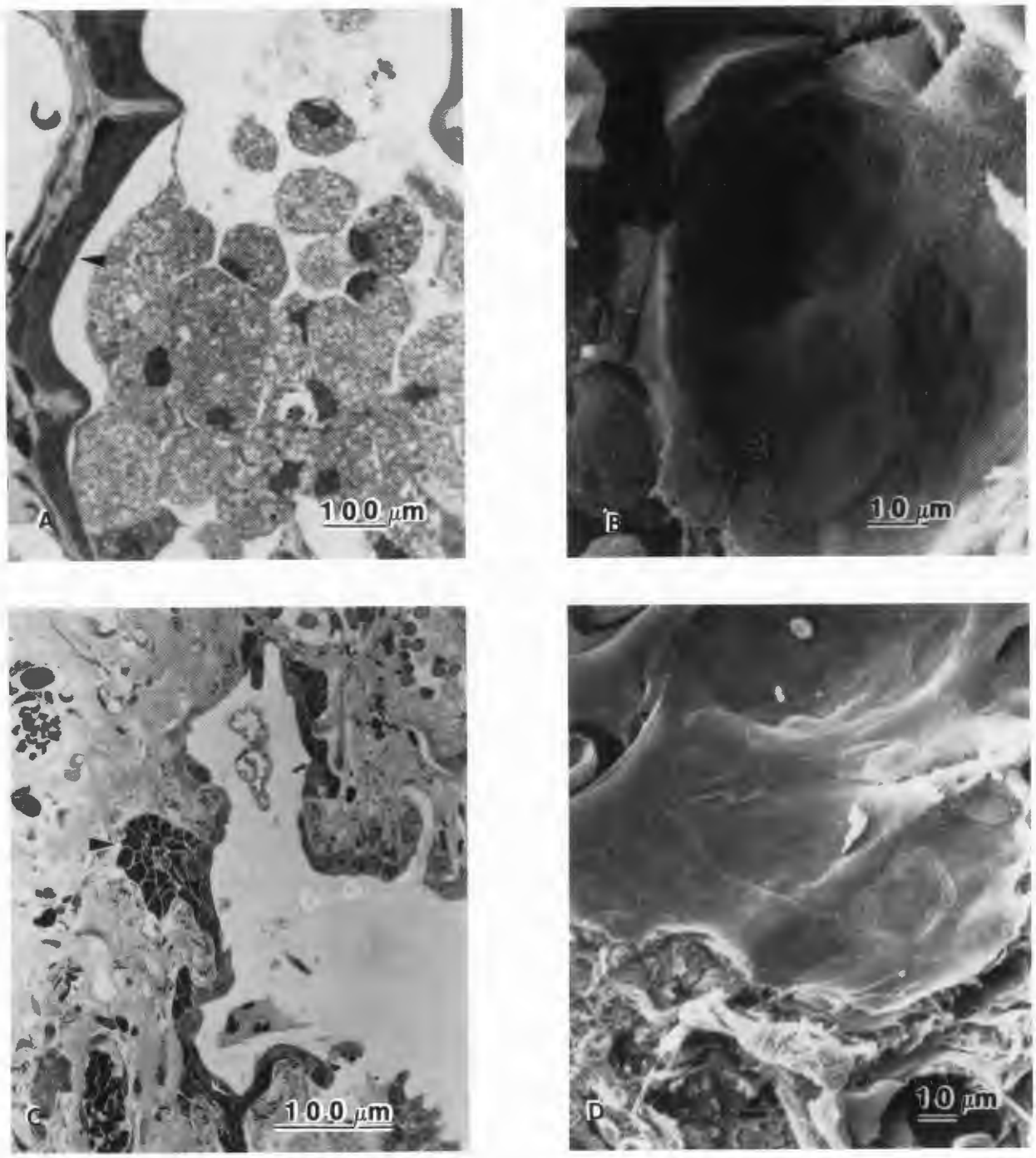

Figure 6. (A) Squamous metaplasia of an alveolus (arrow) and histiocyte accumulation in the air space at 400 days; (B) SEM view of alveolar squamous metaplasia at 600 days; (C) foci of about 20 squamous metaplastic cells (arrow) invading thickened, fibrotic alveolar wall at 500 days; and (D) SEM view of squamous metaplasia in region of severe alveolar fibrosis at 450 days, after inhalation of $^{239}PuO_2$.

and destruction of alveolar architecture (Figure 4 D).

Hyperplasia of type II alveolar epithelial cells was seen by 28 days, becoming more evident by 60-90 days after exposure. Type II cells were often enlarged and contained bizarre and enlarged lamellar bodies (Figures 5 A and 5 B). Occasional type II cells were observed with what appeared to be cilia when examined with the light microscope. Alveolar bronchiolarization first appeared at 120 days after exposure, usually associated with focal inflammatory

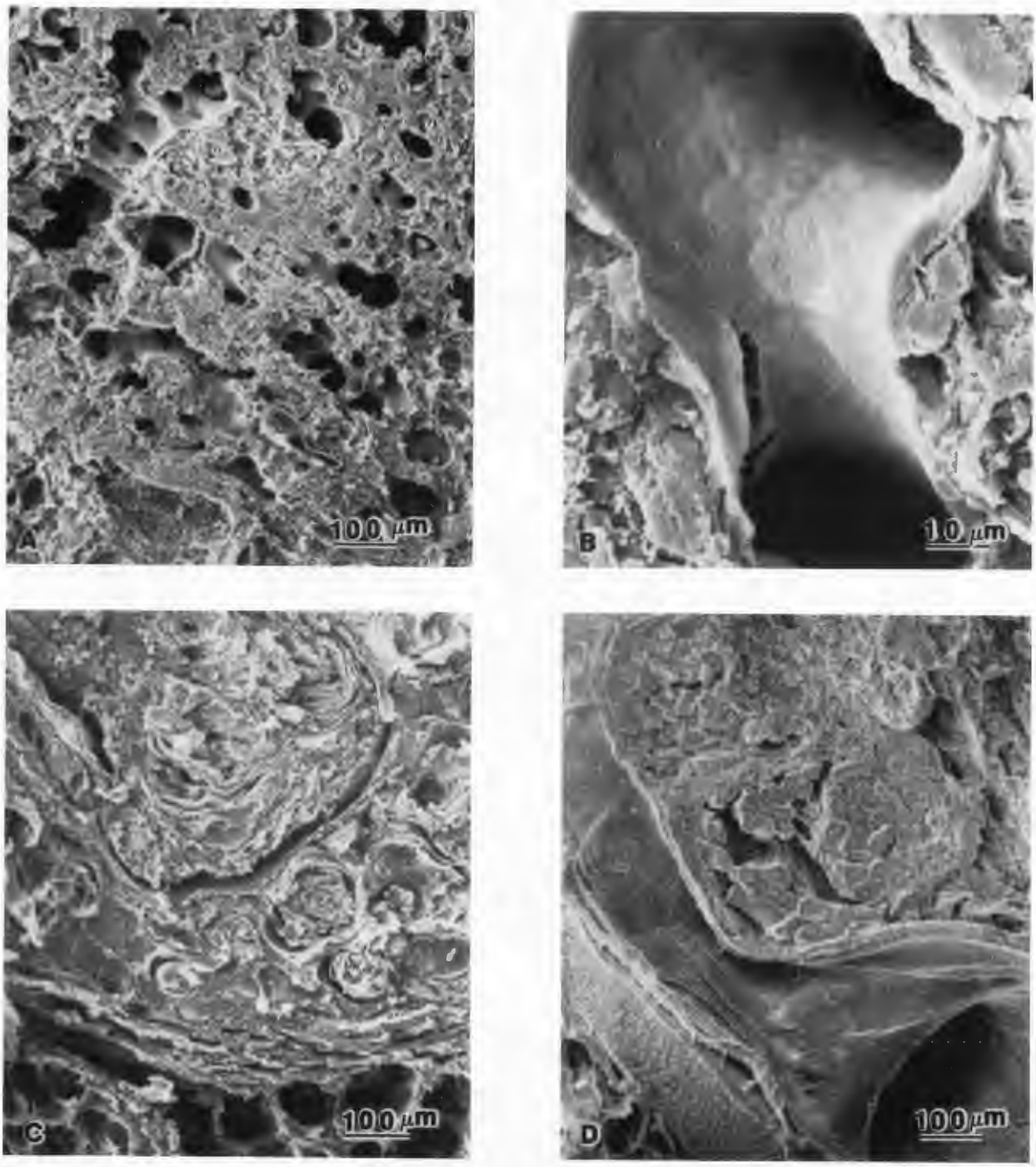

Figure 7. (A) and (B, at higher magnification) Extensive alveolar fibrosis and squamous metaplasia of alveoli and terminal bronchioles at 650 days; (C) squamous carcinoma at 550 days; and (D) adenocarcinoma at 500 days, after inhalation of $^{239}PuO_2$.

and/or fibrotic lesions due to plutonium particle aggregation. Both ciliated and nonciliated cells were found growing along alveolar walls often adjacent to terminal bronchioles and extending at distances from particle aggregates (Figures 5 C and 5 D). At times longer than 180 days, in regions of Pu aggregates, the alveolar walls were sometimes covered by either a cuboidal, nonciliated epithelial surface or by a layered squamous epithelial surface (Figures 6 A and 6 B). Small focal areas of rapidly proliferating squamous metaplasia formed in fibrotic, thickened alveolar walls (Figures 6 C and 6 D), which appear to

eventually develop into squamous carcinoma (Figure 7 C). Pulmonary adenocarcinomas (Figure 7 D) appear at later times than do squamous carcinomas (Table 1).

Discussion

The spatial-temporal, dose distribution pattern in the lung following inhalation of $^{239}PuO_2$ is an important determinant of pulmonary carcinogenesis since emitted alpha particles release their energy in small volumes of lung tissue around each deposited particle. Transmission and SEM autoradiography have been used to visualize inhaled Pu particles within structures of the lung (Sanders and Adee, 1970; Sanders, 1969; Lauhala et al., 1988). SEM autoradiography has been used to quantitate inhaled Pu particle distribution in the lung (Sanders et al., 1989).

Inhaled $^{239}PuO_2$ particles of respirable size are initially deposited in the alveoli in a random, uniform fashion as mostly single particles. About 80% of the cumulative lung dose from inhaled plutonium is delivered during the first few months after exposure (Sanders et al., 1988b). Single, submicron sized $^{239}PuO_2$ particles are incapable of illiciting inflammatory and fibrotic responses. Lung depositions sufficiently high to cause aggregation of Pu particles in individual macrophages are associated with a decrease in early, macrophage-related alveolar clearance of plutonium, and an overall decrease in alveolar macrophage numbers (Morgan et al., 1984; Moores et al, 1986; Sanders, 1972). However, increased numbers of macrophages and other inflammatory cells are seen in focal regions of Pu aggregation within a few months after exposure. These focal, high radiation zones result in focal inflammation, fibrosis and epithelial hyperplasia, metaplasia and neoplasia. Pu particle aggregation has also been described in hamsters (Rhoads et al., 1982; Sanders, 1977), beagle dogs (McShane et al., 1980), and mice (Nicholls et al., 1986).

There are two phases in radiation-induced lung injury: pneumonitis and fibrosis. Radiation pneumonitis and fibrosis responses to external X-and gamma irradiation seen in rats, mice and hamsters are similar to responses seen with instilled or inhaled alpha and beta emitters, except that inhaled radionuclides produce more focal lesions than are seen with external irradiation of lung. Early alveolar reactions to Pu particle aggregates are cell death, inflammation (comprising normal macrophages and histiocytes), type II cell hyperplasia and alveolar wall fibrosis (Heppleston and Young, 1985; Sanders et al., 1971). Similar changes have been observed in irradiated hamster and mouse lung (Woodruff et al., 1977; Maisin et al., 1982; Nicholls et al., 1986). However, the mouse responds to inhaled $^{239}PuO_2$ differently than the rat, with the mouse exhibiting a greater proliferation of mononuclear cells in the alveolar interstitium and a more pronounced type II alveolar epithelial response (Nicholls et al., 1986; Heppleston and Young, 1985).

Pulmonary fibrosis is seen after a 6 month latency period following inhalation of $^{239}PuO_2$ or acute X-or gamma irradiation (Travis and Down, 1981; Coggle et al., 1986; Metivier et al., 1978). The latent period between inhalation exposure and the histological appearance of fibrosis is dependent upon the ability of alveolar epithelial and endothelial cells to replace damaged and killed cells. Loss of cells along either side of the basement membrane in the alveolar wall, along with depressed type II cell repair may enhance interstitial fibrosis (Adamson et al., 1970; Gross, 1981). There is a continuing difference of opinion as to the roles of capillary endothelium and type II cells in radiation pneumonitis and fibrosis (Coggle et al., 1986).

A maximal increase in proliferation of alveolar cells is seen by 60 days postexposure, decreasing gradually to control levels by about 400 days; proliferation, however, in regions of Pu aggregates remains high at all times (unpublished data). A significantly increased proliferation of type II cells is seen following external irradiation of the lung following a latent period of several weeks (Adamson et al., 1970; Adamson and Bowden, 1983; Gross et al., 1987; Coultas et al., 1981). Type I cells are quite radiosensitive, being replaced by proliferating type II cells which then normally redifferentiate to form type I cells (Adamson et al., 1970). The total lung volume distribution or percentage distribution of type II cells is not changed in the rat lung following inhalation of $^{239}PuO_2$ (ILB, 5.9 kBq) at 120-350 days after exposure when examining the whole lung (Rhoads et al., 1981). However, type II cell proliferation in response to continuing injury to type I cells is high in regions of Pu particle aggregation, leading to type II cell hyperplasia and alveolar cuboidal and squamous metaplasia. Type II cell proliferation, if excessive and chronic may also lead to the development of lung tumors (Gross et al., 1987; Masse, 1980).

Of particular interest are doses delivered to nonciliated bronchiolar epithelium since this tissue is thought to be the origin of many pulmonary carcinomas seen in rats after inhalation of $^{239}PuO_2$ (Masse, 198). These cells experience a proliferative response to injury as well as neoplastic transformation. About 5 times more radiation dose was delivered to the bronchiolar epithelium from Pu particles found in peribronchiolar alveoli than from particles found on the bronchiolar surface. Bronchiolar epithelial proliferation appears in two phases. The first phase was seen at 15 days after exposure associated with early clearance of deposited Pu particles from the bronchiolar surfaces. The second proliferative phase, which reached a maximum at 250 days after exposure, appeared associated with Pu particle aggregation in peribronchiolar alveoli (unpublished data). Both type II alveolar epithelium and nonciliated bronchiolar epithelium in terminal bronchioles may participate in alveolar bronchiolarization, squamous metaplasia and carcinoma formation.

Focal alveolar bronchiolarization lesions were usually adjacent or associated with large Pu particle aggregates of sufficient radiation intensity to produce focal inflammatory and fibrotic lesions. Bronchiolarization lesions were comprised of the different cell types (ciliated and nonciliated bronchiolar cells) growing on surfaces of adjacent alveoli. Alveolar bronchiolarization was similar to that seen with nonradioactive irritative dusts such as crystalline silica or volcanic ash (Heppleston, 1963; Sanders et al., 1983), and may be an early dysplastic lesion in the development of metaplasia and pulmonary carcinomas (Masse, 1980). Pu particle aggregates provides the optimum conditions for lung tumor induction at total lung doses greater than 1 Gy by accelerating the

proliferation of initiated bronchiolar and alveolar epithelial cells.

Acknowledgements

This study was supported by the U.S. Department of Energy under Contract DE-AC06-76RLO 1830.

References

Adamson IYR, Bowden DH, Wyatt JP (1970) A pathway to pulmonary fibrosis: An ultrastructural study of mouse and rat following radiation to the whole body and hemithorax. Amer. J. Pathol. 58, 481-498.

Adamson IYR, Bowden DH (1983) Endothelial injury and repair in radiation-induced pulmonary fibrosis. Amer. J. Pathol. 112, 224-230.

Coggle E, Lambert BE, Moores SR (1986) Radiation effects in the lung. Environ. Health Persepct. 70, 261-291.

Coultas PG, Ahier RG, Field SB (1981) Effects of neutron and X irradiation on cell proliferation in mouse lung. Radiat. Res. 85, 516-528.

Gross NJ (1981) The pathogenesis of radiation-induced lung damage. Lung 159, 115-125.

Gross NJ, Narina KR, Colletti-Squinto L (1987) Replicative activity of lung type 2 cells following X irradiation. Radiat. Res. 111, 143-150.

Heppleston AG (1963) The disposal of inhaled particulate matter: A unifying hypothesis. Amer. J. Pathol. 42, 119-135.

Heppleston AG, Young AE (1985) Population and ultrastructural changes in murine alveolar cells following $^{239}PuO_2$ inhalation. J. Path. 146, 155-166.

Lauhala KE, Sanders CL, McDonald KE (1988) Scanning electron microscopic autoradiography of lung. Scanning Microscopy 2, 1631-1634.

Lisco H (1959) Autoradiographic and histopathologic studies in radiation carcinogenesis of the lung. Lab. Invest. 8, 162-170.

Maisin JR, Van Gorp U, de Saint-Georges L (1982) The ultrastructure of the lung after exposure to ionizing radiation as seen by transmission and scanning electron microscope. Scanning Electron Microsc. 1982; 1: 403-412.

Masse R (1980) Histogenesis of lung tumors induced in rats by inhalation of alpha emitters: An overview. In Pulmonary Toxicology of Respirable Particles, CONF-791002, NTIS, Springfield, VA, 498-521.

McDowell EM, Trump BF (1976) Histologic fixatives suitable for diagnostic light and electron microscopy. Arch. Pathol. Lab. Med. 100, 405-414.

McShane JF, Dagle GE, Park JF (1980) Pulmonary distribution of inhaled $^{239}PuO_2$ in dogs. In: Pulmonary Toxicology of Respirable Particles, CONF-791002, NTIS, Springfield, VA, 248-255.

Metivier H, Masse R, Legendre N, Lafuma J (1978) Pulmonary connective tissue modification induced by internal alpha irradiation. 1. Effect of time and dose on alterations following inhalation of plutonium-239 dioxide in rat.. Radiat. Res. 75, 385-396.

Moores SL, Talbot RJ, Evans N, Lambert BE (1986) Macrophage depletion in mouse lung following inhalation of $^{239}PuO_2$. Radiat. Res. 105, 387-404.

Morgan A, Black A, Moores SR (1984) Retention of ^{239}Pu in the mouse lung and estimation of consequent dose following inhalation of sized $^{239}PuO_2$. Radiat. Res. 99, 272-284.

Nicholls LG, Moores SR, Talbot RJ, de Saint-Georges L (1986) Fibrotic and pneumonitic changes in the mouse lung following inhalation of $^{239}PuO_2$. In: AERE R 11795, United Kingdom Atomic Energy Authority, Harwell, Oxfordshire, England.

Rhoads K, Mahaffey JA, Sanders CL (1981) A morphometric study of rat and hamster lung following inhalation of $^{239}PuO_2$. Radiat. Res. 88, 266-279.

Rhoads K, Mahaffey JA, Sanders CL (1982) Distribution of inhaled $^{239}PuO_2$ in rat and hamster lung. Health Phys. 42, 645-656.

Rhoads K, Mahaffey JA, Sanders CL (1983) Dosimetry and response in rat pulmonary epithelium following inhalation of $^{239}PuO_2$. In: Current Concepts in Lung Dosimetry, CONF-820492-Pt.1, NTIS, Springfield, VA, 59.

Sanders CL, (1969) The distribution of inhaled $^{239}PuO_2$ particles within pulmonary macrophages. Arch. Environ. Health 18, 904-912.

Sanders CL, Adee RR (1970) Ultrastructural localization of inhaled $^{239}PuO_2$ in alveolar epithelium and macrophages. Health Phys. 18, 293-296.

Sanders CL, Adee RR, Jackson TA (1971) Fine structure of alveolar area in the lung following inhalation of $^{239}PuO_2$. Arch. Environ. Health 22, 525-533.

Sanders CL (1972) Deposition patterns and toxicity of transuranium elements in lung. Health Phys. 22, 607-615.

Sanders CL (1977) Inhalation toxicology of $^{238}PuO_2$ and $^{239}PuO_2$ in Syrian golden hamsters. Radiat. Res. 70, 334-344.

Sanders CL, Rhoads K, Mahaffey JA (1983) Long-term reactivity of lung and mediastinal lymph nodes following intratracheal instillation of sandy loam soil or Mount St. Helens volcanic ash. Environ. Res. 32, 188-198.

Sanders CL, McDonald KE, Killand BW, Mahaffey JA, Cannon WA (1986) Low-level lifespan studies with inhaled $^{239}PuO_2$ in rats. In: Life-Span Radiation Effects Studies in Animals: What Can They Tell Us?, CONF-830591, NTIS, Springfield, VA, 429-449.

Sanders CL, McDonald KE, Mahaffey JA (1988a) Lung tumor response to inhaled Pu and its implications to radiation protection. Health Phys. 55, 455-462.

Sanders CL, McDonald KE, Lauhala KE (1988b) Promotion of pulmonary carcinogenesis by plutonium particle aggregation following inhalation of $^{239}PuO_2$. Radiat. Res. 116, 393-405.

Sanders CL, McDonald KE, Lauhala KE (1988c) Scanning electron microscopy: Aggregation of inhaled $^{239}PuO_2$. Intern. J. Rad. Biol. 54, 115-121.

Sanders CL, Lauhala KE, McDonald KE (1989) Quantitative scanning electron microscopic autoradiography of inhaled $^{239}PuO_2$. Health Phys. 56, 321-325.

Travis EL, Down JD (1981) Repair in mouse lung after split doses of X-rays. Radiat. Res. 87, 166-174.

Woodruff KH, Leith JT, Smith P, Havens V, Lyman JT, Howard J, Tobias CA (1977) Irradiation damage in hamster lung. In: Pulmonary Macrophage and Epithelial Cells, CONF-760927, NTIS, Springfield, VA, 533-551.

Discussion With Reviewers

D.P. Penney: What was the fate of the macrophage population throughout the study?
Authors: There is a general decline in pulmonary macrophage numbers following inhalation of $^{239}PuO_2$ (Sanders. 1969, text reference). However, macrophage numbers associated with Pu particle aggregates and focal inflammatory lesions are greatly increased.

E.L. Travis: Do you have further evidence that pulmonary adenocarcinomas appear later than squamous carcinomas?
Authors: Lung tumor type and latency period are functions of radiation dose from inhaled $^{239}PuO_2$. At doses less than 1 Gy adenocarcinoma appears before squamous carcinoma, while at doses greater than 1 Gy adeno carcinoma appears after squamous carcinoma (C.L. Sanders, R.R. Adee, and K. Rhoads. 1977. Life history of plutonium dioxide in the lung: From macrophage to carcinoma. In, Pulmonary Macrophage and Epithelial Cells, CONF-760297, NTIS, Springfield, VA, pp. 451-462). The relationship between lung tumor type, latency and radiation dose is apparently due to the formation of large Pu aggregates at high ILB values (Sanders et al., 1988b, text reference).

D.E. Schraufnagel: Squamous metaplasia may be a response of the epithelium that results from stimuli that also cause carcinoma. How do you know that squamous metaplasia eventually will develop into squamous carcinoma?
Authors: Squamous metaplasia from areas of focal inflammation and fibrosis typically precedes the development of squamous carcinoma in the rat, not only for inhaled radionuclides but for non-radioactive irritative particles in the lung, such as silica. Temporally, qualitatively and quantitatively, it has been shown the squamous metaplasia is a precursor of squamous carcinoma.

J.B. Reitan: What is the relative biological effectiveness (RBE) for inhaled radionuclides emitting high LET alpha-radiation compared to low LET beta, gamma radiations?
Authors: In rats, the RBE for mortality from radiation pneumonitis/fibrosis is about 10 for inhaled alpha-emitters, while for lung tumors the RBE ranges from 20 to 50.

J.B. Reitan: How much of the pulmonary toxicity is due to radiation and how much is due to chemical toxicity and mechanical irritation of the dust particles?
Authors: ^{239}Pu has a specific activity of 16 mg/mCi, while $^{239}PuO_2$ has a density of about 11 g/cm^3. High-fired (calcined at 750°C for 2 hours) $^{239}PuO_2$ is very insoluble in biological tissues. Low solubility and mass of deposited PuO_2 particles (1.6 micrograms) rules out a role for mechanical or chemical toxicity.

J.B. Reitan: The $^{239}PuO_2$ aggregates in your experiments represent very active hot-spots. Your data are of relevance regarding the fate of inhaled alpha-emitting radon daughters and following inhalation of hot particles from Chernobyl with a mixture of alpha, beta, and gamma-emitting radionuclides. These later particles were rather large. Do you think your data on the aggregation of ^{239}Pu have any relevance for the discussion of the biological effects of Chernobyl particles?
Authors: Our results with inhaled transuranics are relevant to the issue of 'hot particles.' The more homogeneous alpha irradiation pattern from inhaled 'soluble' $^{241}AmO_2$ and $^{244}CmO_2$ resulted in a maximum lung tumor incidence of about 30% at a dose of 2-3 Gy. The more nonhomogeneous lung dose pattern from inhaled 'insoluble' $^{238}PuO_2$ and $^{239}PuO_2$ produced a maximum lung tumor incidence of about 80% at 8-10 Gy. The difference in dose-tumor response between these two dose distribution patterns is seen in the formation of particle aggregates with PuO_2 and associated greater incidence of squamous carcinoma and hemangiosarcoma. Adenocarcinomas predominate with a uniform alpha irradiation pattern in the lung, whose risk may be estimated by a quadratic function or a threshold. On the other hand, squamous carcinoma and hemangiosarcoma formation exhibit a threshold at 1 Gy and 5 Gy, respectively (C.L. Sanders and J.A. Mahaffey. 1979. Inhalation toxicology of transuranics in rodents. In, Biological Implications of Radionuclides Released from Nuclear Industries, IAEA Symposium, Vol. I, Vienna, Austria, pp. 89-104; and Sanders et al., 1988a, text reference).